

Origin of Long-Term Storage Stability and Nitric Oxide Release Behavior of CarboSil Polymer Doped with S-Nitroso-N-acetyl-D-penicillamine

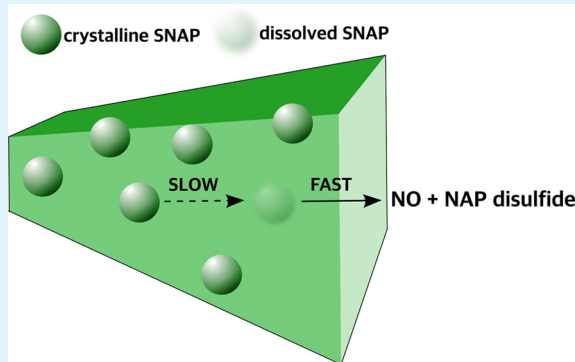
Yaqi Wo,[†] Zi Li,[†] Elizabeth J. Brisbois,[‡] Alessandro Colletta,[†] Jianfeng Wu,[§] Terry C. Major,[‡] Chuanwu Xi,[§] Robert H. Bartlett,[‡] Adam J. Matzger,[†] and Mark E. Meyerhoff^{§,†}

[†]Department of Chemistry, [‡]Department of Surgery, University of Michigan Medical Center, and [§]Department of Environmental Health Sciences, University of Michigan, Ann Arbor, Michigan 48109, United States

S Supporting Information

ABSTRACT: The prolonged and localized delivery of nitric oxide (NO), a potent antithrombotic and antimicrobial agent, has many potential biomedical applications. In this work, the origin of the long-term storage stability and sustained NO release mechanism of S-nitroso-N-acetyl-D-penicillamine (SNAP)-doped CarboSil 20 80A polymer, a biomedical thermoplastic silicone-polycarbonate-urethane, is explored. Long-term (22 days) localized NO release is achieved by utilizing a cross-linked silicone rubber as topcoats, which can greatly reduce the amount of SNAP, NAP, and NAP disulfide leaching from the SNAP-doped CarboSil films, as measured by LC-MS. Raman spectroscopy and powder X-ray diffraction characterization of SNAP-doped CarboSil films demonstrate that a polymer-crystal composite is formed during the solvent evaporation process when SNAP exceeds its solubility in CarboSil (ca. 3.4–4.0 wt %). Further, when exceeding this solubility threshold, SNAP exists in an orthorhombic crystal form within the bulk of the polymer. The proposed mechanism of sustained NO release in SNAP-doped CarboSil is that the solubilized SNAP in the polymer matrix decomposes and releases NO, primarily in the water-rich regions near the polymer/solution interface, and the dissolved SNAP in the bulk polymeric phase becomes unsaturated, resulting in the dissolution of crystalline SNAP within the bulk of the polymer. This is a very slow process that ultimately leads to NO release at the physiological flux levels for >3 weeks. The increased stability of SNAP within CarboSil is attributed to the intermolecular hydrogen bonds between the SNAP molecules that crystallize. This crystallization also plays a key role in maintaining RSNO stability within the CarboSil polymer for >8 months at 37 °C (88.5% remains). Further, intravascular catheters fabricated with this new material are demonstrated to significantly decrease the formation of *Staphylococcus aureus* biofilm (a leading cause of nosocomial bloodstream infections) (*in vitro*) over a 7 day period, with 5 log units reduction of viable cell count on catheter surfaces. It is also shown that the NO release catheters can greatly reduce thrombus formation on the catheter surfaces during 7 h implantation in rabbit veins, when compared to the control catheters fabricated without SNAP. These results suggest that the SNAP-doped CarboSil system is a very attractive new composite material for creating long-term NO release medical devices with increased stability and biocompatibility.

KEYWORDS: nitric oxide, controlled release, S-nitroso-N-acetyl-D-penicillamine (SNAP), polymer-crystal composite, antimicrobial catheters, thromboresistance, biocompatibility



INTRODUCTION

Blood-contacting biomedical devices ranging from simple catheters to complex extracorporeal life support systems¹ are central for everyday medical care. For example, the use of intravascular catheters, which enables direct vascular access, is crucial for patient diagnosis and treatment. However, despite substantial efforts to better understand blood/surface interactions, complications like pulmonary embolism, stroke, and deep vein thrombosis are still associated with the use of indwelling blood-contacting medical devices.² In a clinical setting, a systemic anticoagulation agent, such as heparin, is often given to patients in order to reduce the risk of surface-

induced thrombus formation.³ However, heparin treatment should be conducted with extreme care, as an inadvertent overdose of heparin can lead to hemorrhage and thrombocytopenia.⁴ Although heparin preferentially binds to antithrombin (ATIII), preventing fibrin formation and hindering the development of the hemostatic plug, platelet activation and reduced platelet count is inevitable when foreign surfaces are in contact with blood for a prolonged period. Moreover, biofilm-

Received: June 1, 2015

Accepted: September 22, 2015

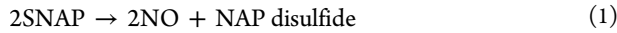
Published: September 22, 2015



associated infections are a significant cause of morbidity and death. *Staphylococcus aureus* (*S. aureus*) is the most prevalent cause of the high incidence of nosocomial bloodstream infections, specifically, biofilm-associated infections on indwelled biomedical devices.^{5,6} *S. aureus* biofilms form embedded matrixes which resist both antimicrobials and host defense, thus leading to chronic infections.⁷ Therefore, new approaches to reduce the possibilities of these complications and to create truly nonthrombogenic and antimicrobial prosthetic surfaces are still needed within the medical community.²

Nitric oxide (NO), the endothelium-derived relaxing factor, is a gaseous signaling molecule that has been extensively studied over the past two decades for its role in inhibiting platelet activation and adhesion, preventing bacterial growth, reducing smooth cell proliferation, regulating complex biological processes, etc.^{8–31} The ubiquity and apparent chemical simplicity of NO have made it a promising therapeutic agent. The production of NO can be accomplished through either enzymatic or nonenzymatic pathways.^{11,32} Nitric oxide either can be synthesized enzymatically by nitric oxide synthase (NOS) that catalyze the conversion of L-arginine to L-citrulline or can be formed nonenzymatically from the reduction of nitrite¹¹ or nitrosothiols. The flux of NO released from a healthy endothelium lining, which constitutes the inner walls of all blood vessels, has been estimated to be between 0.5 and 4.0×10^{-10} mol cm⁻² min⁻¹.^{3,10,33,34} Therefore, a potential approach to increase the hemocompatibility of blood-contacting devices is to develop polymeric materials or coatings with sustained NO release at this physiological flux level. Indeed, it has been demonstrated that surfaces capable of releasing NO at these levels can significantly reduce thrombus formation on the surface of implantable chemical sensors,³⁵ intravascular catheters,^{14,15} as well as extracorporeal circuits (ECC).^{3,10,33}

Since NO is highly reactive under physiological conditions and has a very short half-life *in vivo*,^{10,36} a wide range of NO donors, such as S-nitrosothiols (RSNO) and N-diaziniumdilates (NONOate), have been used to prepare NO releasing polymeric matrixes. Such NO donors have been incorporated into various polymers, including polyethylene glycol,³⁷ Pluronic F127 hydrogel,¹² polyurethanes,³⁸ poly(dimethylsiloxane) (PDMS),⁹ xerogel,³⁹ and poly(vinyl chloride),²³ and these materials can provide continuous and localized NO delivery to specific sites of interest. S-Nitrosoglutathione (GSNO), S-nitrosohemoglobin (SNO-Hb), and other endogenous RSNOs are considered NO donors *in vivo*. However, in recent years, researchers have studied synthetic RSNOs, such as S-nitroso-N-acetylpenicillamine (SNAP).^{9,10,18} SNAP is a synthetic tertiary RSNO, and it is more stable than most endogenous primary RSNOs due to the steric hindrance of the sulfur atom.^{40,41} SNAP, like other RSNOs, can decompose and release NO via thermal decomposition, metal ion catalysis (e.g., Cu⁺), and photolysis when the light energy corresponds with the SNAP absorption bands at 340 nm and/or 590 nm (see eq 1 for overall reaction).^{10,42}



Previous work by our group has suggested that SNAP is stable when doped within low water uptake polymers, such as Elast-eon E2As, a siloxane-base polyurethane elastomer.¹⁰ Doping SNAP into the E2As polymer using a solvent evaporation method produced a homogeneous and transparent film, which exhibits relatively high stability during shelf life

studies (82% of the initial SNAP remains after 2 months of dry storage at 37 °C).¹⁰ However, the details of the NO release mechanism from SNAP within the polymer phase and the reason SNAP is so stable in certain polymer materials still remains unclear.

In this study, three different SNAP-doped biomedical grade polymers, including CarboSil 20 80A (a thermoplastic silicone-polycarbonate-urethane with a mix of soft segments of poly(dimethylsiloxane) and polycarbonate as well as a hard segment of methylene diphenyl isocyanate (MDI)), Elast-eon S-325 (a copolymer of mixed soft segments of poly(dimethylsiloxane) and poly(hexamethylene oxide) as well as the MDI hard segment), and silicone rubber (poly(dimethylsiloxane)) are investigated and further evaluated for their ability to store SNAP for extended periods at 37 °C. CarboSil 20 80A possesses the innate biocompatibility and biostability of conventional silicone elastomers but has the processing capability and toughness of thermoplastic polycarbonates-urethanes. Therefore, the SNAP/CarboSil system is further examined for its NO releasing properties, and leaching of SNAP as well as concomitant NAP and NAP disulfide (NAP dimers) with time from the polymer phase into the PBS soaking buffer. Raman spectroscopy and powder X-ray diffraction are utilized to conduct *in situ* solid-state analysis of the SNAP/CarboSil system to better understand the origin of the high stability and long-term NO release properties of this new composite material. Further, catheters fabricated with SNAP-doped CarboSil polymer are evaluated for their efficacy in reducing microbial biofilm formation after 7 days of exposure to flowing media containing *S. aureus*, the common bacteria that causes intravascular infections within a drip-flow bioreactor. Finally, these NO release catheters are also investigated for their potential as antithrombotic devices via 7 h implantation within the veins of rabbits.

EXPERIMENTAL SECTION

Cumulative SNAP, NAP, and NAP Disulfide Leaching from SNAP-Doped CarboSil Polymer Films Immersed in PBS. Ten wt % SNAP-doped CarboSil films with no topcoat, 2 layers of CarboSil topcoats, and 2 layers of SR topcoats, respectively, were fabricated (see the Supporting Information) and placed in individual vials containing 1 mL of 10 mM PBS, pH 7.4, with 100 μM EDTA to minimize trace metal catalyzed decomposition of SNAP. All films were incubated in the dark at 37 °C at all times. After various time points, aliquots (15 μL) of the individual soaking solutions were analyzed by liquid chromatography–tandem mass spectrometry (6520 Accurate-Mass Q-TOF LC/MS, Agilent Technologies, CA) for quantification of SNAP, NAP, and NAP disulfide present in the soaking solution. The studies were conducted using a reversed-phase column (ZORBAX RRHD Eclipse Plus C18, 2.1 × 50 mm). The gradient was obtained with eluent A (water with 0.1% formic acid) and eluent B (95% acetonitrile, 0.1% formic acid). After sample injection (15 μL), a linear change of eluent mixtures from 100% A to 0% A over 10 min was carried out with a flow rate of 0.4 mL/min. The mass spectrometer used electrospray ionization in the negative ion mode, and the detected species were [M – H]⁻. All films were placed in fresh PBS buffer immediately after each measurement while the previous soaking solutions were analyzed. The results were compared between films with different topcoats. The amount of total SNAP ([SNAP]_{total}) that had diffused into the PBS after time *t* was calculated as follows: [SNAP]_{total} = [SNAP]_{*t*} + [NAP]_{*t*} + 2 × [NAP disulfide]_{*t*}. The amount of total SNAP leached into the buffer was compared with the initial amount SNAP in the polymer film.

Cumulative NO Release from SNAP-Doped CarboSil Films/Catheters. Nitric oxide release from the polymer films or catheters was measured using a Sievers chemiluminescence Nitric Oxide

Analyzer (NOA) 280i (Boulder, CO). For example, a 10 wt % SNAP-doped CarboSil film with 2 SR topcoats was placed in the sample vial containing 4 mL of 10 mM PBS, pH 7.4, with 100 μ M EDTA at 37 °C to mimic the physiological conditions. Nitric oxide was continuously generated and immediately purged and swept into the chemiluminescence detection chamber by N₂ sweeping gas and bubbler. All films were placed in fresh PBS buffer during NO release measurements and incubated at 37 °C in the absence of ambient light after each measurement. Cumulative NO release ([NO]_{total}) of a given SNAP-doped CarboSil film after various time points was determined by the sum of the NO release amount in fresh PBS measured by NOA ([NO]_{NOA}) and total amount of SNAP ([SNAP]_{total}) leached into previous soaking solutions: [NO]_{total} = [NO]_{NOA} + [SNAP]_{total}. Cumulative NO release ([NO]_{total}) was also compared with the initial amount SNAP in the polymer film.

Raman Spectroscopy Characterization. Raman spectra were collected by using a Renishaw inVia Raman microscope equipped with a Leica microscope, a RenCam CCD detector, and a 633 nm laser employing an 1800 lines/nm grating and a 50 μ m slit. Spectra were obtained using the WiRE 3.4 software package. Calibration was performed using a silicon standard in static mode. Full spectra of blank CarboSil (without SNAP), pure SNAP crystals, and 15 wt % SNAP-doped CarboSil were collected through an Olympus SLMPlan 20 \times objective in extended scan mode in the range of 100–4000 cm^{-1} and further analyzed by ACD/SpecManager Version 12.01 software from Advanced Chemistry Development, Inc. For Raman mapping characterization, SNAP-doped CarboSil samples were cut into thin strips and laid down on the stage with the cross section facing upward. Raman cross-section mapping data were obtained by using an Olympus SLMPlan 100 \times objective in combination with an automatic Renishaw MS20 encoded stage in static scan mode. The exposure time was 40 s with a static scan centered at 720 cm^{-1} . The mapping data were analyzed using the Wire 3.4 software package component direct classical least-squares (DCLS) analysis routines with the full spectra of blank CarboSil and pure SNAP crystals as references.

Powder X-ray Diffraction (PXRD) Measurements. Powder X-ray diffraction (PXRD) patterns of SNAP-doped (1–15 wt %) and blank CarboSil films (without topcoats) were collected at room temperature using a Rigaku R-Axis Spider diffractometer with an image plate detector and graphite monochromated Cu-K α radiation (λ = 1.54187 Å) at 40 kV and 44 mA. Synthesized SNAP crystals were finely ground to eliminate preferred orientation, whereas blank CarboSil and SNAP-doped CarboSil samples were cut into cubes with dimensions of approximately 250 μ m. All samples were mounted on a CryoLoop using heavy mineral oil, and images were collected for 15 min with a 0.3 mm collimator. The ω -axis was oscillated between 120° and 180° at 1°/s, the ϕ -axis was rotated at 10°/s, and the χ -axis was fixed at 45°. The obtained images were integrated from 2.5° to 70° with a 0.1° step size in AreaMax 2.0 software from Rigaku. All powder patterns were processed using Jade 9 XRD Pattern Processing, Identification & Quantification analysis software from Materials Data, Inc. The simulated powder patterns of monoclinic and orthorhombic SNAP crystals were calculated in Mercury 3.3 from the CCDC and were compared with the experimental SNAP powder pattern in Jade 9. Linear least-squares regression for quantitation of peak area ratios versus doped-SNAP weight percentage was performed in MATLAB. PXRD measurements of 5 and 15 wt % SNAP/CarboSil film (both freshly made and 10 days old under ambient environment at RT) were taken and compared.

Preparation of SNAP-Doped CarboSil Catheters. The 20 wt % SNAP-doped CarboSil catheters and CarboSil control catheters employed in the *in vitro* antibiofilm and/or *in vivo* rabbit experiments were prepared by dip-coating on 2.0 mm or 1.1 mm diameter straight stainless steel mandrels (McMaster-Carr, IL). The catheters consisted of SNAP-doped CarboSil inner layers and SR outer layers on both inside and outside surfaces of the catheters. For the drip-flow reactor biofilm experiments (*in vitro*), the final catheters had an i.d. of 2.0 mm and an o.d. of 4.0 mm. However, because of the size limitation of rabbit veins, catheters with 1.1 mm i.d. and 2.2 mm o.d. were

fabricated for the *in vivo* rabbit experiments. Details of the catheter fabrication procedures are reported in the [Supporting Information](#) file.

In Vitro Characterization of SNAP-Doped CarboSil Catheters against Microbial Biofilm. *S. aureus* ATCC 25923 was used as model strain in this study. Biofilm was developed onto the surfaces of control and NO release catheters for 7 days using a drip-flow biofilm reactor (Biosurface Technologies Corp., Bozeman, MT).¹⁵ Details of the microbiology procedures used in relation to the studies reported here are provided in the [Supporting Information](#) file.

In Vivo Characterization of SNAP-Doped CarboSil Catheters in the Veins of Rabbits. Five centimeter lengths of the catheters (one SNAP and one control) were inserted into the jugular veins of rabbits for 7 h to test the hemocompatibility of both catheters. The animal experiment details are provided in the [Supporting Information](#) file. At the end of the experiments, the catheters were carefully removed from the veins, and the thrombus was left intact on the catheter surface and quantitated using ImageJ imaging software provided by the National Institutes of Health (NIH).

Statistical Analysis. All experiments were conducted in triplicate. Data are all expressed as mean \pm SEM (standard error of the mean). Comparison of means using student's *t* test was utilized to analyze the statistical differences between SNAP-doped catheters and control catheters. Values of *p* < 0.05 were considered statistically significant for all tests.

RESULTS AND DISCUSSION

Preliminary Shelf Life Study of Various SNAP-Doped Biomedical Grade Polymer Films. Three biomedical grade polymers (CarboSil, E5-32S, and SR) with low water uptake (see Table S1 in the [Supporting Information](#)) were chosen as matrixes for incorporating SNAP. Ten wt % SNAP-doped polymer films were prepared to evaluate their shelf life during dry storage. To simulate the actual storage and/or shipping environments, the SNAP-doped SR, E5-32S, and CarboSil films were stored in the dark with desiccant at 37 °C over a period of 8 months. The amount of SNAP remaining in different polymer films was determined at various time points to find the best polymer matrix for maintaining SNAP functionality during storage. The SNAP remaining in the film was decomposed through both the Cu(I) mediated catalytic decomposition pathway and the photoinitiated decomposition pathway by the broad-spectrum 100 W halogen light source. The corresponding NO release measured by the NOA was integrated to determine the total amount of SNAP present in the polymer. The results indicate that SNAP is the most stable in the CarboSil polymer matrix, with 88.5 \pm 4.3% of the initial SNAP remaining after 8 months, compared to 86.8 \pm 4.9% in SR and 68.3 \pm 3.2% in E5-32S (see [Figure 1](#)). Though the conventional silicone elastomer also exhibits equivalent stability, its lack of processability together with the prolonged polymer curing process (for cross-linking to occur) makes CarboSil a more promising material in terms of NO release properties.

Ethylene Oxide (EtO) Sterilization of Various SNAP-Doped Biomedical Grade Polymer Films. Ethylene oxide sterilization is a routine procedure for sterilizing clinical appliances inside hospitals, during which the devices are subjected to high temperature and high humidity level.^{43,44} Ten wt % of SNAP-doped SR, E5-32S, and CarboSil were sterilized in order to evaluate the SNAP stability in these materials when undergoing ETO sterilization. The results parallel the shelf life studies, indicating that SNAP is most stable within the CarboSil polymer matrix. Indeed, the CarboSil films maintain 91.8 \pm 3.2% of the initial SNAP after ETO sterilization, compared to 82.7 \pm 3.8% for the E5-32S films and 78.7 \pm 3.1% for the SR

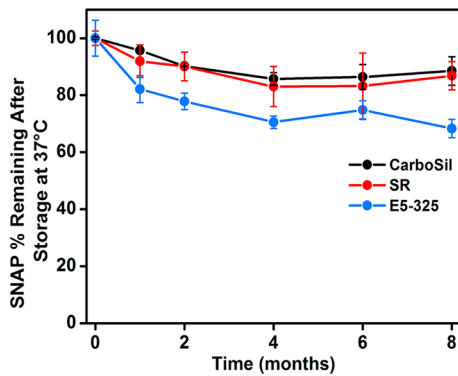


Figure 1. Shelf life study of 10 wt % SNAP-doped CarboSil, SR, and E5-325 films stored dry (with desiccant) in the dark at 37 °C. The SNAP remaining in the films after various time points is determined and compared with the initial level. Data are mean \pm SEM ($n = 3$).

films (see Table S2). These data suggest that the SNAP-doped CarboSil polymer matrix is the most attractive of all formulations as a NO release material for fundamental studies and eventually for potential biomedical applications.

Cumulative Leaching and NO Release of SNAP-Doped CarboSil Films. Although SNAP is reported to be slightly hydrophobic and should preferentially stay within the polymer phase,⁴⁵ some SNAP is likely to diffuse from the polymer to the soaking solution. Thus, *in vitro* studies were conducted with SNAP-doped CarboSil films to examine the effects of different

topcoat polymers by analyzing the amount of total SNAP leached into the PBS during soaking. Ten wt % SNAP-doped CarboSil films with no topcoat, 2 layers of CarboSil topcoat, and 2 layers of SR topcoat were soaked in 1 mL of PBS at 37 °C. Although SNAP can absorb light in the UV range (see Figure S1 in the *Supporting Information*),^{37,42} it is not practical to quantify its decomposition species (e.g., NAP and NAP disulfide) by UV-Vis.^{37,46} Therefore, the concentrations of SNAP, NAP, and NAP disulfide in PBS solution buffers at each time point were monitored by LC-MS. Standard solutions of NAP, NAP disulfide, and SNAP (1, 5, 10, 20, 40, and 60 μ M) were prepared and analyzed for the individual elution times and concentration-peak area calibration curves (see Figure S2 in the *Supporting Information*). The elution times of NAP, NAP disulfide, and SNAP from the C18 column are determined to be 3.45, 4.25, and 4.5 min, respectively, which correspond with the increasing log P values of three molecules (-0.07 , 0.01 , and 0.40 , respectively). The log P values were calculated using Marvin Sketch software, where a higher value means greater lipophilicity and hence a longer retention time. Ten wt % SNAP films initially contain ca. 450 nmol of SNAP per mg of polymer. When SNAP films are in contact with the soaking solutions, water starts to diffuse into the polymer outer surface; SNAP begins to leach into the soaking buffer; and at the same time, SNAP (both from the PBS buffer and within the polymer) starts to release NO and form the NAP disulfide byproduct. The detection of NAP thiolate ion in the soaking solutions can be from two possible sources. It is known that, for

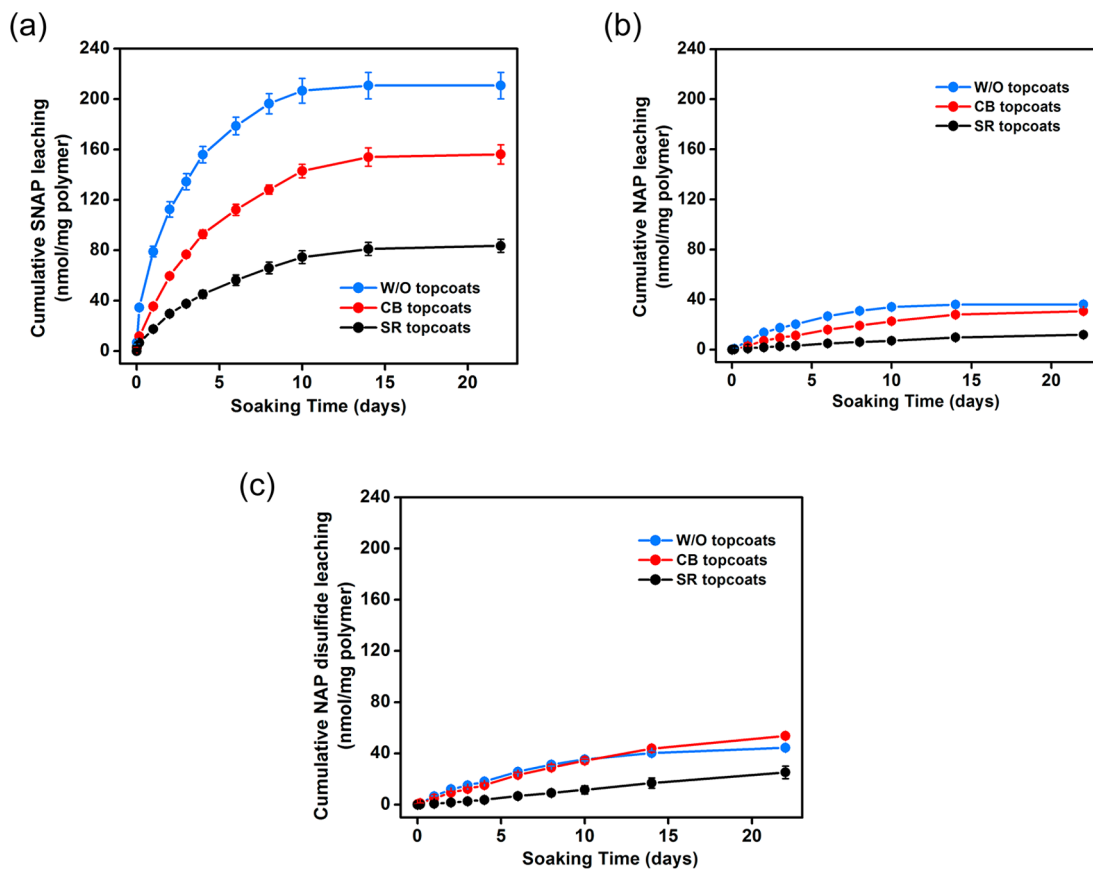


Figure 2. Cumulative leaching of SNAP (a), NAP (b), and NAP disulfide (c) into 1 mL of PBS (soaking buffer) from 10 wt % SNAP-doped CarboSil films with different coating conditions: without topcoats, CarboSil topcoats, and SR topcoats, over the period of 22 days, at 37 °C in the dark. Data are mean \pm SEM ($n = 3$).

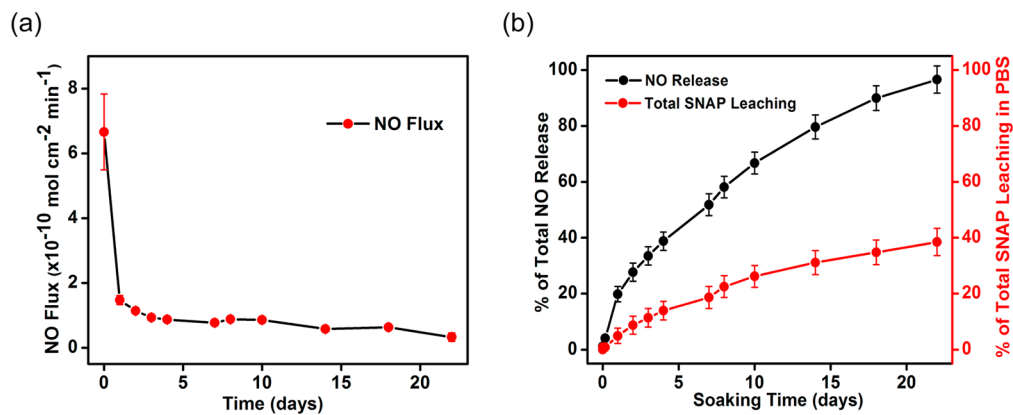


Figure 3. (a) NO flux from 10 wt % SNAP-doped CarboSil films with SR topcoats in PBS at 37 °C for 22 days. Data are mean \pm SEM ($n = 3$). (b) Comparison of total NO release and total SNAP leaching (sum of SNAP, NAP, and disulfide species) from the 10 wt % SNAP-doped CarboSil films with SR coatings soaking in PBS at 37 °C. The cumulative/total NO release comes from the thermal decomposition of the SNAP in polymer phase as well as the SNAP leached into the buffer. The SNAP leached in PBS accounts for 38.5% of the total NO release. Data are mean \pm SEM ($n = 3$).

solid RSNO samples, contamination of thiols is likely and such thiols can react with the trace amount of Cu(II) in solution and form Cu(I) (eq 2). Then, Cu(I), acting as a catalyst, can react with RSNOs (e.g., SNAP), and form RS[−] (e.g., NAP thiolate) and Cu(II) (eq 3).^{47,48} Alternatively, it is conceivable that small amounts of thiolate can be generated by hydrolysis of RSNOs (eq 4).⁴⁸



As shown in Figure 2a, 47% of the initial SNAP (210 nmol/mg polymer) diffuses out of the CarboSil films without any topcoat over the period of 22 days, compared to 35% for the films with the CarboSil topcoat and only 19% for the films with the SR topcoat. For each type of film, the rate of SNAP leaching is the fastest in the first few hours, and then significantly lower amounts of SNAP continue to diffuse into the PBS over sequential days. The SR topcoat, which is a cross-linked polymer, can reduce the amount of SNAP diffusion into the soaking solution better than the non-cross-linked CarboSil topcoat. Similar leaching patterns are observed for the NAP and NAP disulfide species from the films with different topcoats (Figure 2b,c). NAP is a widely used chelating and detoxifying agent for treatment of heavy metal poisoning (e.g., mercury, cadmium, and arsenic, etc.).^{49–54} Indeed, it hastens the excretion of poisons out of human body without inducing toxic effects, and it represents a protective measure against free radical induced organ injury.⁵³ Therefore, it is reasonable to believe that small amounts NAP and/or the dimer of NAP (NAP disulfide) emitted from the polymer into the contacting buffer or blood would not likely cause any toxic response in clinical applications.¹⁰

The 10 wt % SNAP-doped CarboSil film with SR topcoats releases NO above 0.5×10^{-10} mol $\text{cm}^{-2} \text{min}^{-1}$, the lower end of endothelial NO flux levels, for more than 3 weeks under physiological conditions (see Figure 3a). A large burst of NO release was observed by the NOA (via chemiluminescence) on day 0 that correlates with the rapid SNAP leaching into the PBS buffer in the first few hours. The cumulative amount of SNAP that releases NO was calculated based on the NOA

measurements and compared to the initial amount doped within the film. The total NO release from polymer films can originate from the SNAP decomposing and releasing NO inside the polymer phase as well as from SNAP molecules that diffuse out of the polymer into the PBS buffer. Assuming that the NAP and NAP disulfide detected in the buffer are reaction products of the original SNAP leached from the polymer, the total amount of SNAP that leaches out after time t should be $[\text{SNAP}]_{\text{total}} = [\text{SNAP}]_t + [\text{NAP}]_t + 2 \times [\text{NAP disulfide}]_t$. Since the films were placed into fresh PBS during NOA measurements, the NO release detected by the NOA can be only attributed to the SNAP decomposing and releasing NO from inside the polymer phase ($[\text{NO}]_{\text{NOA}}$) (assuming the amount of SNAP leaching during the measurement was negligible). Therefore, the total NO release ($[\text{NO}]_{\text{total}}$) from the polymer film is $[\text{NO}]_{\text{total}} = [\text{NO}]_{\text{NOA}} + [\text{SNAP}]_{\text{total}}$, which was compared with the initial SNAP in the CarboSil film. As shown in Figure 3b, the total moles of SNAP ($[\text{SNAP}]_{\text{total}}$) leached out over 22 days, the time period of the leaching experiment, is approximately 38.5% of the total NO released ($[\text{NO}]_{\text{total}}$) and, therefore, more than 60% of the total NO is, in fact, released from the polymer phase. This suggests that the leaching process is much slower than the rate of NO release from the polymers, so it is likely that, after the first day, NO release from within the polymer (primarily in the water-rich regions near the outer surfaces of the polymers) is the primary source of NO emission. The ability of the SNAP/CarboSil polymer system to deliver localized NO continuously and sufficiently to sites of interest makes it a very promising material for biomedical applications.

Solid-State Analysis of SNAP-Doped CarboSil Polymer Systems.

To better understand the fundamental reasons for which SNAP is so stable in CarboSil and is able to release NO for 3 weeks, a series of solid phase characterization has been conducted. Films of 5 wt % SNAP-doped CarboSil and blank CarboSil were viewed under a polarized optical microscope. Distinguished crystalline patterns were found in the SNAP/CarboSil film in comparison with the blank film (see Figure S3 in the Supporting Information). Therefore, it is hypothesized that SNAP crystallized in the polymer matrix during the solvent evaporation process, as opposed to all dissolving in the polymer and forming a homogeneous matrix as previously suggested.¹⁰ We further compared the Raman spectra of SNAP crystals, blank CarboSil film, and 15 wt % SNAP/CarboSil film. The

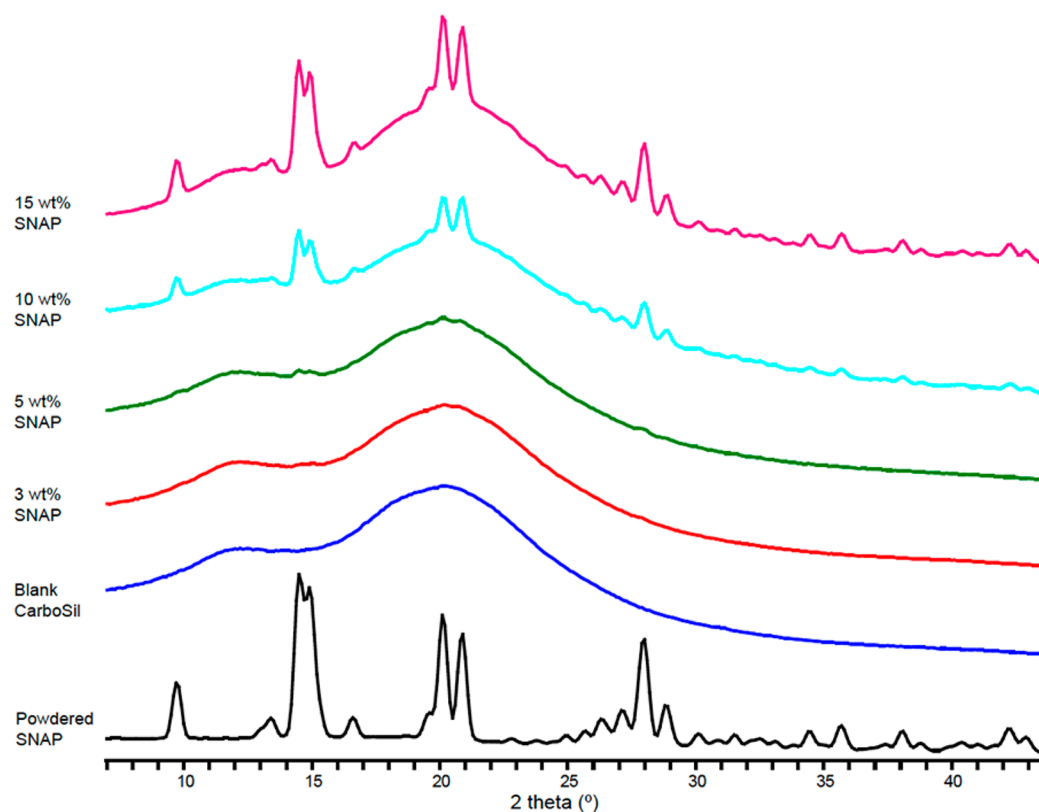


Figure 4. Representative PXRD patterns of SNAP powder, blank CarboSil, and SNAP-doped CarboSil film samples of different weight percentages (1–15 wt %) were tested. Sample peaks were able to be clearly distinguished when the wt % SNAP doping is no less than 4 wt %.

spectrum of 15 wt % SNAP/CarboSil (Figure S4) showed characteristic peaks of both CarboSil and crystalline SNAP that further substantiates the existence of crystalline SNAP within the polymer film.

In order to identify the form of crystalline SNAP detected in the Raman spectroscopy characterization, powder X-ray diffraction (PXRD) analysis of the synthesized SNAP crystals was conducted, and the results agree with the patterns of the orthorhombic SNAP reported in the literature (see Figure S5). It has been suggested that, in orthorhombic SNAP, one SNAP molecule can form 4 intermolecular hydrogen bonds with 4 surrounding SNAP molecules (Figure S6).⁵⁵ The PXRD results of SNAP-doped CarboSil films (1–15 wt %) indicate that the characteristic film diffraction patterns are convolutions of blank CarboSil and the crystalline SNAP powder patterns (see Figure 4). The results also suggest that, as the amount of doped SNAP increases (for films with greater than 4 wt % SNAP), the intensity of orthorhombic SNAP peaks in the obtained PXRD pattern is enhanced, indicating a greater percentage of crystalline SNAP within the polymer films. However, SNAP peaks could barely be detected in PXRD patterns for samples with <4 wt % doped SNAP, indicating an apparent threshold for formation of the crystalline form of SNAP within CarboSil. Since all SNAP-doped CarboSil films (including those with <4 wt %) have a light green color, it is speculated that SNAP partially dissolves in the polymer, forming a polymer solution, and any excess SNAP beyond the polymer solubility limit crystallizes in the orthorhombic form during the THF evaporation and embeds in the polymer. This explanation is in agreement with the Raman spectroscopy and PXRD results that orthorhombic SNAP crystals are detected only when the SNAP concentration exceeds the solubility of SNAP in the

CarboSil polymer. To calculate the SNAP solubility in the CarboSil polymer, a linear least-squares regression was conducted (see the *Supporting Information*) using three main PXRD peaks. The calculated solubility is 3.6, 3.5, and 3.9 wt %, respectively (see Figure S7), indicating that the solubility of SNAP in CarboSil was ca. 3.4–4.0 wt %.

Characterizing the stabilities of SNAP-doped CarboSil films using PXRD further verifies the dissolution hypothesis. We compared the PXRD patterns of freshly prepared 5 and 15 wt % SNAP-doped CarboSil samples as well as the samples stored under ambient light at room temperature for 10 days under the same conditions. We hypothesize that the solubilized SNAP behaves as a solute, dissolving in the CarboSil polymer that acts as the solvent, and it is less stable at room temperature and decomposes faster than the crystalline SNAP. As the solubilized SNAP in the polymer decomposes and the SNAP in the polymer is under saturation, the crystalline SNAP is driven to gradually dissolve into the CarboSil polymer. For 5 wt % fresh samples, most of the SNAP added during preparation is dissolved in the polymer, which is labile and more likely to decompose via thermal decomposition. However, for the 15 wt % SNAP films, most of the SNAP in the film (ca. 11–12 wt %) is stabilized by the intermolecular hydrogen bonding.⁵⁵ The percentage of SNAP remaining in the 5 and 15 wt % films after 10 days under ambient light is 19.8 and 83.2 wt % of the initial amount, respectively. The attenuation of orthorhombic SNAP peaks in 5 wt % SNAP-doped CarboSil films relative to the fresh samples is indeed much greater than that of the 15 wt % samples (see Figure S8) where the SNAP peak changes are almost undetectable, thus validating our hypothesis.

Intermolecular hydrogen bonding in the SNAP crystals is one of the key reasons for the elevated stability of SNAP-doped

CarboSil films during dry storage for 8 months. In addition, as a tertiary nitrosothiol, the SNAP molecule itself is more stable with respect to the loss of NO than other primary and secondary RSNOs due to the steric hindrance effect imposed by the gem methyl group on the dimerization of the radicals that leads to the formation of the sulfur bridge^{10,40,41,45} and the hindered rotation of the R—S—N—O linkage at room temperature.⁵⁵ The literature also suggests that the acetamide group in SNAP plays a key role in increasing the S—NO bond strength and reducing the NO lability.⁴⁶ Moreover, it has also been reported that the viscosity of the polymer imposes an important cage effect on the S—NO bond cleavage and radical pair formation. Specifically, the restricted mobility of soluble SNAP molecules in the CarboSil microenvironment may favor the recombination of the primary radicals rather than radicals escaping from the solvent cage.^{10,12,37} Therefore, doping SNAP into the polymer represents a viable option for storage and handling for long-term NO release applications. Further studies comparing SNAP solubility in different polymer matrixes and examining the relationship between the SNAP crystallization/dissolution process and the stability of SNAP in certain polymers could be quite useful in designing additional NO release polymers with enhanced stability and long-term shelf life.

Lastly, Raman mapping characterization using static scans was employed to determine the 2D representation of the SNAP crystal distribution in 3 and 5 wt % SNAP-doped CarboSil films. The green spots in Figure 5 represent regions where the

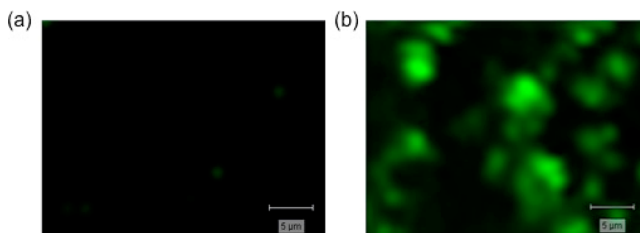


Figure 5. Raman mapping results for fitting of (a) 3 wt % and (b) 5 wt % SNAP-doped CarboSil with pure orthorhombic SNAP spectrum as the reference under 100× objective. Green represents areas fitting the crystalline SNAP spectrum.

orthorhombic SNAP peaks are detected and are found in large quantities only in the 5 wt % SNAP/CarboSil film, but not in 3 wt % films. This finding correlates with the PXRD peak area fitting results that indicate that the solubility of SNAP in polymer is ca. 3.4–4.0 wt %. However, the exact grain sizes of the SNAP crystals could not yet be quantified by this method because the focal depth of the laser is likely to exceed the grain size of the crystal. Thus, the green spots could represent crystals from both the surface and deeper within the polymer phase, which results in difficulty in distinguishing any individual crystal from overlaid crystals.

In Vitro Antibiofilm Experiments. In order to generate NO release (at the higher end of the normal physiological flux level) for longer periods, 20 wt % SNAP-doped CarboSil catheters were prepared as described in the **Experimental Section**. These devices can release physiological levels of NO for 28 days at 37 °C (see Figure S9 in the **Supporting Information**). Because stable NO releasing devices can abate bacterial adhesion and colonization associated with catheterization, we examined the antibiofilm properties of catheter

segments with *S. aureus* for 7 days in a drip-flow bioreactor at 37 °C. The drip-flow bioreactor was chosen because it promotes the growth of the bacteria that grows at the air–liquid interface, which mimics the condition of the surface of indwelling intravascular catheters. Results for 7 day *S. aureus* biofilms shows a 5 logarithmic unit reduction in viable cell count on the surfaces of NO release catheters segments when compared to the control segments (see Figure 6a). This finding

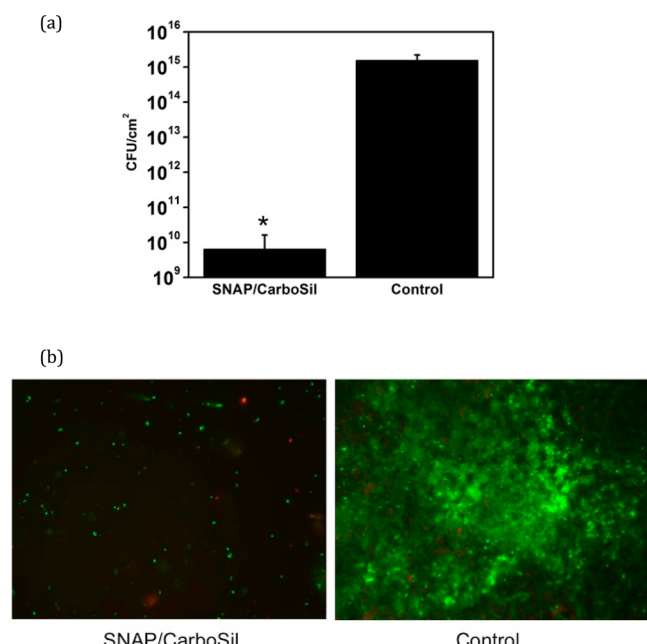


Figure 6. *S. aureus* biofilms developed on catheter segments in a drip-flow bioreactor for 7 days. (a) Plate count of the number of viable bacteria adhered to the catheter surface. (b) Representative fluorescence images with oil immersion 60× objective lens of the biofilms on the surface of the catheter.

is further corroborated by the fluorescent images (Figure 6b), which illustrates the live/dead bacteria as well as the bacterial surface coverage on the surfaces of both catheters, respectively. These results demonstrate that the SNAP/CarboSil catheter provides an approach that can potentially reduce/prevent catheter-related bloodstream infections.

In Vivo Antithrombotic Experiments in Rabbits. In order to demonstrate the potential benefits of using SNAP-doped CarboSil polymer as a thromboresistant material, acute 7 h rabbit experiments were conducted to study the effect of NO release from CarboSil catheters on the thrombus formation area. The NO release from the SNAP/CarboSil catheter maintains an average flux of approximately 5.5×10^{-10} mol $\text{cm}^{-2} \text{ min}^{-1}$ for 7 h at 37 °C (see Figure S10 in the **Supporting Information**). One SNAP/CarboSil and one control catheter (non-SNAP) were placed into the external jugular veins of each rabbit for 7 h. Owing to the very slow loss of SNAP from the catheter reservoir (given the composite nature of the material), the dose of SNAP leached from the catheters is significantly below the threshold that can induce the adverse reactions.¹⁰

After 7 h of implantation, the catheters were carefully removed from the rabbit veins, leaving the thrombus formation intact on the surface. To determine whether the NO release reduced the clotting on the catheter surface, digital images of the catheter surfaces were taken, and the two-dimensional (2D) representation of the thrombus area was quantitated using

ImageJ software from the NIH. As shown in Figure 7, the thrombus formation is significantly reduced for the SNAP/CarboSil catheters.

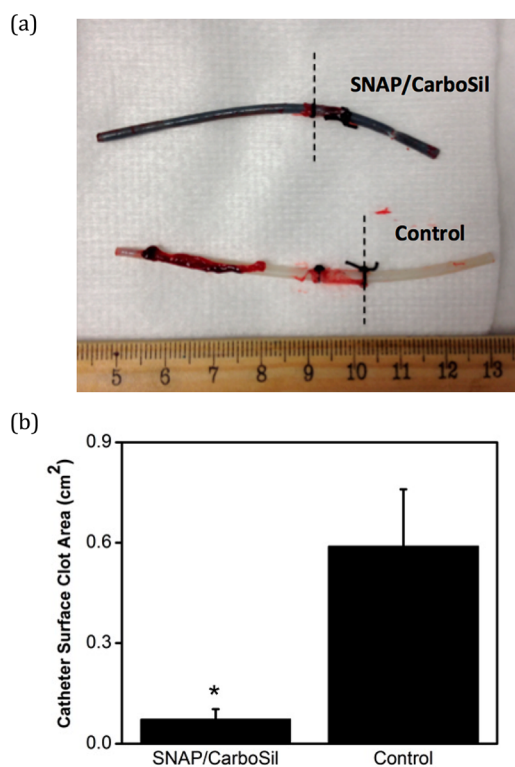


Figure 7. (a) Five cm of the catheters (left of the dash line) were inserted into the rabbit external jugular veins for 7 h. Representative pictures of thrombus formation on the SNAP/CarboSil and control catheters after removal from veins. (b) Two-dimensional representation of clot area (cm^2) on SNAP/CarboSil and control catheters in rabbit veins for 7 h, as quantitated using ImageJ software from NIH. Data are mean \pm SEM ($n = 3$). * = $p < 0.05$, SNAP/CarboSil vs control catheters.

CarboSil catheters with NO release ability when compared to the controls ($n = 3$ rabbit experiments). The SNAP/CarboSil catheters were also examined for NO release rates via chemiluminescence after explantation, and they still exhibit an average flux of $3.8 \pm 0.2 \text{ mol cm}^{-2} \text{ min}^{-1}$. This clearly demonstrates that the localized NO release from the catheter surface can significantly reduce platelet activation and thrombus formation.

CONCLUSIONS

In this study, we have shown that SNAP doped into the CarboSil 20 80A polymer forms a polymer–crystal composite during solvent evaporation and can locally release NO over a 22 day period via thermal decomposition. Utilizing a cross-linked silicone rubber topcoat can greatly reduce the amount of SNAP, NAP, and NAP disulfide leaching as measured by LC–MS. The 10 wt % SNAP/CarboSil has excellent stability during the 8 month shelf life study at 37°C as well as during ethylene oxide sterilization, where 88.5% and 91.8% of the initial SNAP remain in the polymer, respectively. These data suggest the practicality of sterilizing, storing, and shipping biomedical devices made with or coated with this material. Raman spectroscopy and PXRD characterization of SNAP-doped CarboSil films demonstrate that the solubility of SNAP in

CarboSil is ca. 3.4–4.0 wt %. However, when the SNAP doping wt % is higher than this solubility threshold, SNAP exists in an orthorhombic crystal form within the bulk of the polymer, in which intermolecular hydrogen bonds between SNAP molecules play a key role in maintaining the RSNO stability and functionality over a long period of time. Solubilized SNAP in the polymer phase behaves like a solute in the solid solution polymer system and is less stable and decomposes faster than the crystalline SNAP. When the solubilized SNAP in polymer decomposes/releases NO and the SNAP within the polymer phase is under saturation, the crystalline SNAP in the bulk of the polymer is driven to gradually dissolve into the polymer and further release NO. The NO release process ceases after 22 days when all the SNAP crystals are depleted. The catheters fabricated with this SNAP composite are shown to exhibit significant antibiofilm properties against *S. aureus*, and such catheters could eventually be used to reduce the rate of nosocomial catheter related bloodstream infections. The SNAP/CarboSil catheters also greatly reduce thrombus formation during 7 h implantation within the veins of rabbits when compared to the corresponding control catheters. Given its excellent stability and long-term NO release capability, the new SNAP-doped CarboSil composite system offers many new opportunities to improve the biocompatibility of biomedical devices for many applications.

ASSOCIATED CONTENT

Supporting Information

The Supporting Information is available free of charge on the ACS Publications website at DOI: 10.1021/acsami.5b07501.

Experiment details on SNAP/CarboSil film and catheter fabrication, film stability study at 37°C , ethylene oxide (EtO) sterilization, *in vitro* antibiofilm studies (including biofilm growth condition, plate counting, and biofilm imaging), and *in vivo* rabbit experiments (PDF)

AUTHOR INFORMATION

Corresponding Author

*E-mail: mmeryho@umich.edu. Phone: (734) 763-5916.

Notes

The authors declare no competing financial interest.

ACKNOWLEDGMENTS

This work was supported by grants from the National Institutes of Health (EB-000783, R41-DK101206-01, and GM106180). We wish to thank DSM for the gift of CarboSil 20 80A polymer and AorTech International for the gift of Elast-eon 5-325 polymer. We also want to thank Ms. Bing Fu for the help with the use of the Matlab software.

REFERENCES

- (1) Ratner, B. D. The Catastrophe Revisited: Blood Compatibility in the 21st Century. *Biomaterials* **2007**, *28*, 5144–5147.
- (2) Suchyta, D. J.; Handa, H.; Meyerhoff, M. E. A Nitric Oxide-Releasing Heparin Conjugate for Delivery of a Combined Anti-platelet/anticoagulant Agent. *Mol. Pharmaceutics* **2014**, *11*, 645–650.
- (3) Handa, H.; Brisbois, E. J.; Major, T. C.; Refahiyyat, L.; Amoako, K. A.; Annich, G. M.; Bartlett, R. H.; Meyerhoff, M. E. In Vitro and in Vivo Study of Sustained Nitric Oxide Release Coating Using Diazeniumdiolate-Doped Poly(vinyl Chloride) Matrix with Poly(lactide-Co-Glycolide) Additive. *J. Mater. Chem. B* **2013**, *1*, 3578–3587.

(4) Robinson, T. M.; Kickler, T. S.; Walker, L. K.; Ness, P.; Bell, W. Effect of Extracorporeal Membrane Oxygenation on Platelets in Newborns. *Crit. Care Med.* **1993**, *21* (7), 1029–1034.

(5) Allan, N. D.; Giare-Patel, K.; Olson, M. E. An in Vivo Rabbit Model for the Evaluation of Antimicrobial Peripherally Inserted Central Catheter to Reduce Microbial Migration and Colonization as Compared to an Uncoated PICC. *J. Biomed. Biotechnol.* **2012**, *2012*, 921617.

(6) Otto, M. Staphylococcal Infections: Mechanisms of Biofilm Maturation and Detachment as Critical Determinants of Pathogenicity. *Annu. Rev. Med.* **2013**, *64*, 175–188.

(7) Kiedrowski, M. R.; Horswill, A. R. New Approaches for Treating Staphylococcal Biofilm Infections. *Ann. N. Y. Acad. Sci.* **2011**, *1241*, 104–121.

(8) Kolluru, G. K.; Shen, X.; Kevil, C. G. A Tale of Two Gases: NO and H₂S, Foes or Friends for Life? *Redox Biol.* **2013**, *1*, 313–318.

(9) Gierke, G. E.; Nielsen, M.; Frost, M. C. S-Nitroso-N-Acetyl-D-Penicillamine Covalently Linked to Polydimethylsiloxane (SNAP-PDMS) for Use as a Controlled Photoinitiated Nitric Oxide Release Polymer. *Sci. Technol. Adv. Mater.* **2011**, *12*, 055007.

(10) Brisbois, E. J.; Handa, H.; Major, T. C.; Bartlett, R. H.; Meyerhoff, M. E. Long-Term Nitric Oxide Release and Elevated Temperature Stability with S-Nitroso-N-Acetylpenicillamine (SNAP)-Doped Elast-Eon E2As Polymer. *Biomaterials* **2013**, *34* (28), 6957–6966.

(11) Kolluru, G. K.; Yuan, S.; Shen, X.; Kevil, C. G. H₂S Regulation of Nitric Oxide Metabolism. *Methods Enzymol.* **2015**, *554*, 271–297.

(12) Shishido, S. M.; Seabra, A. B.; Loh, W.; de Oliveira, M. G. Thermal and Photochemical Nitric Oxide Release from S-Nitrosothiols Incorporated in Pluronic F127 Gel: Potential Uses for Local and Controlled Nitric Oxide Release. *Biomaterials* **2003**, *24* (20), 3543–3553.

(13) Höfler, L.; Koley, D.; Wu, J.; Xi, C.; Meyerhoff, M. E. Electromodulated Release of Nitric Oxide through Polymer Material from Reservoir of Inorganic Nitrite Salt. *RSC Adv.* **2012**, *2* (17), 6765–6767.

(14) Ren, H.; Colletta, A.; Koley, D.; Wu, J.; Xi, C.; Major, T. C.; Bartlett, R. H.; Meyerhoff, M. E. Thromboresistant/Anti-Biofilm Catheters via Electrochemically Modulated Nitric Oxide Release. *Bioelectrochemistry* **2015**, *104*, 10–16.

(15) Ren, H.; Wu, J.; Xi, C.; Lehnert, N.; Major, T.; Bartlett, R. H.; Meyerhoff, M. E. Electrochemically Modulated Nitric Oxide (NO) Releasing Biomedical Devices via copper(II)-tri(2-Pyridylmethyl)amine Mediated Reduction of Nitrite. *ACS Appl. Mater. Interfaces* **2014**, *6* (6), 3779–3783.

(16) Bohl, K. S.; West, J. L. Nitric Oxide-Generating Polymers Reduce Platelet Adhesion and Smooth Muscle Cell Proliferation. *Biomaterials* **2000**, *21*, 2273–2278.

(17) Brisbois, E. J.; Bayliss, J.; Wu, J.; Major, T. C.; Xi, C.; Wang, S. C.; Bartlett, R. H.; Handa, H.; Meyerhoff, M. E. Optimized Polymeric Film-Based Nitric Oxide Delivery Inhibits Bacterial Growth in a Mouse Burn Wound Model. *Acta Biomater.* **2014**, *10*, 4136–4142.

(18) Brisbois, E. J.; Davis, R. P.; Jones, A. M.; Major, T. C.; Bartlett, R. H.; Meyerhoff, M. E.; Handa, H. Reduction in Thrombosis and Bacterial Adhesion with 7 Day Implantation of S-Nitroso-N-Acetylpenicillamine (SNAP)-Doped Elast-Eon E2As Catheters in Sheep. *J. Mater. Chem. B* **2015**, *3*, 1639–1645.

(19) Frost, M. C.; Reynolds, M. M.; Meyerhoff, M. E. Polymers Incorporating Nitric Oxide Releasing/generating Substances for Improved Biocompatibility of Blood-Contacting Medical Devices. *Biomaterials* **2005**, *26* (14), 1685–1693.

(20) Reynolds, M. M.; Frost, M. C.; Meyerhoff, M. E. Nitric Oxide-Releasing Hydrophobic Polymers: Preparation, Characterization, and Potential Biomedical Applications. *Free Radical Biol. Med.* **2004**, *37* (7), 926–936.

(21) Reynolds, M. M.; Saavedra, J. E.; Showalter, B. M.; Valdez, C. a; Shanklin, A. P.; Oh, B. K.; Keefer, L. K.; Meyerhoff, M. E. Tailored Synthesis of Nitric Oxide-Releasing Polyurethanes Using O-Protected Diazieniumdiolated Chain Extenders. *J. Mater. Chem.* **2010**, *20* (15), 3107–2114.

(22) Reynolds, M. M.; Hrabie, J. a; Oh, B. K.; Politis, J. K.; Citro, M. L.; Keefer, L. K.; Meyerhoff, M. E. Nitric Oxide Releasing Polyurethanes with Covalently Linked Diazieniumdiolated Secondary Amines. *Biomacromolecules* **2006**, *7* (3), 987–994.

(23) Simões, M. M.; de Oliveira, M. G. Poly(vinyl Alcohol) Films for Topical Delivery of S-Nitrosoglutathione: Effect of Freezing-Thawing on the Diffusion Properties. *J. Biomed. Mater. Res., Part B* **2010**, *93* (2), 416–424.

(24) Seabra, a B.; Fitzpatrick, a; Paul, J.; De Oliveira, M. G.; Weller, R. Topically Applied S-Nitrosothiol-Containing Hydrogels as Experimental and Pharmacological Nitric Oxide Donors in Human Skin. *Br. J. Dermatol.* **2004**, *151* (5), 977–983.

(25) Li, Y.; Lee, P. Controlled Nitric Oxide Delivery Platform Based on S-Nitrosothiol Conjugated Interpolymer Complexes for Diabetic Wound Healing. *Mol. Pharmaceutics* **2010**, *7*, 254–266.

(26) Keyaerts, E.; Vijgen, L.; Chen, L.; Maes, P.; Hedenstierna, G.; Van Ranst, M. Inhibition of SARS-Co coronavirus In Vitro by S-Nitroso-N-Acetylpenicillamine, a Nitric Oxide Donor Compound. *Int. J. Infect. Dis.* **2004**, *8* (4), 223–226.

(27) Hetrick, E. M.; Schoenfisch, M. H. Analytical Chemistry of Nitric Oxide. *Annu. Rev. Anal. Chem.* **2009**, *2*, 409–433.

(28) Riccio, D. A.; Schoenfisch, M. H. Nitric Oxide Release: Part I. Macromolecular Scaffolds. *Chem. Soc. Rev.* **2012**, *41*, 3731–3741.

(29) Colletta, A.; Wu, J.; Wo, Y.; Kappler, M.; Chen, H.; Xi, C.; Meyerhoff, M. E. S -Nitroso- N -Acetylpenicillamine (SNAP) Impregnated Silicone Foley Catheters: A Potential Biomaterial/Device To Prevent Catheter-Associated Urinary Tract Infections. *ACS Biomater. Sci. Eng.* **2015**, *1*, 416–424.

(30) Carpenter, A. W.; Schoenfisch, M. H. Nitric Oxide Release: Part II. Therapeutic Applications. *Chem. Soc. Rev.* **2012**, *41* (10), 3742–3752.

(31) Coneski, P. N.; Schoenfisch, M. H. Nitric Oxide Release: Part III. Measurement and Reporting. *Chem. Soc. Rev.* **2012**, *41* (10), 3753–3758.

(32) Lundberg, J. O.; Weitzberg, E.; Gladwin, M. T. The Nitrate–Nitrite–Nitric Oxide Pathway in Physiology and Therapeutics. *Nat. Rev. Drug Discovery* **2008**, *7* (3), 156–167.

(33) Handa, H.; Major, T. C.; Brisbois, E. J.; Amoako, K. A.; Meyerhoff, M. E.; Bartlett, R. H. Hemocompatibility Comparison of Biomedical Grade Polymers Using Rabbit Thrombogenicity Model for Preparing Nonthrombogenic Nitric Oxide Releasing Surfaces. *J. Mater. Chem. B* **2014**, *2* (8), 1059–1067.

(34) Vaughn, M.; Kuo, L.; Liao, J. Estimation of Nitric Oxide Production and Reaction Rates in Tissue by Use of a Mathematical Model. *J. Cell. Physiol.* **1998**, *274* (6), H2163–H2176.

(35) Wu, Y.; Meyerhoff, M. E. Nitric Oxide-Releasing/Generating Polymers for the Development of Implantable Chemical Sensors with Enhanced Biocompatibility. *Talanta* **2008**, *75* (3), 642–650.

(36) Hakim, T. S.; Sugimori, K.; Camporesi, E. M.; Anderson, G. Half-Life of Nitric Oxide in Aqueous Solutions with and Without Haemoglobin. *Physiol. Meas.* **1996**, *17* (4), 267–277.

(37) Shishido, S. M.; de Oliveira, M. G. Polyethylene Glycol Matrix Reduces the Rates of Photochemical and Thermal Release of Nitric Oxide from S-Nitroso-N-Acetylcysteine. *Photochem. Photobiol.* **2000**, *71* (3), 273–280.

(38) Coneski, P. N.; Schoenfisch, M. H. Synthesis of Nitric Oxide-Releasing Polyurethanes with S-Nitrosothiol-Containing Hard and Soft Segments. *Polym. Chem.* **2011**, *2*, 906.

(39) Riccio, D. A.; Coneski, P. N.; Nichols, S. P.; Broadnax, A. D.; Schoenfisch, M. H. Photoinitiated Nitric Oxide-Releasing Tertiary S-Nitrosothiol-Modified Xerogels. *ACS Appl. Mater. Interfaces* **2012**, *4* (2), 796–804.

(40) Wang, P. G.; Xian, M.; Tang, X.; Wu, X.; Wen, Z.; Cai, T.; Janczuk, A. J. Nitric Oxide Donors: Chemical Activities and Biological Applications. *Chem. Rev.* **2002**, *102* (4), 1091–1134.

(41) Lin, C. E.; Richardson, S. K.; Wang, W.; Wang, T.; Garvey, D. S. Preparation of Functionalized Tertiary Thiols and Nitrosothiols. *Tetrahedron* **2006**, *62* (May), 8410–8418.

(42) Frost, M. C.; Meyerhoff, M. E. Controlled Photoinitiated Release of Nitric Oxide from Polymer Films Containing S-Nitroso-N-Acetyl-DL-Penicillamine Derivatized Fumed Silica Filler. *J. Am. Chem. Soc.* **2004**, *126* (5), 1348–1349.

(43) Mendes, G. C.; Brandão, T. R.; Silva, C. L. Ethylene Oxide Sterilization of Medical Devices: A Review. *Am. J. Infect. Control* **2007**, *35*, 574–581.

(44) Matthews, I. P.; Gibson, C.; Samuel, A. H. Sterilization of Implantable Devices. *Clin. Mater.* **1994**, *15*, 191–215.

(45) Megson, I. L.; Morton, S.; Greig, I. R.; Mazzei, F. A.; Field, R. A.; Butler, A. R.; Caron, G.; Gasco, A.; Fruttero, R.; Webb, D. J. N-Substituted Analogues of S-Nitroso-N-Acetyl-D,L-Penicillamine: Chemical Stability and Prolonged Nitric Oxide Mediated Vaso-dilatation in Isolated Rat Femoral Arteries. *Br. J. Pharmacol.* **1999**, *126* (3), 639–648.

(46) De Oliveira, M. G.; Shishido, S. M.; Seabra, A. B.; Morgan, N. H. Thermal Stability of Primary S-Nitrosothiols: Roles of Autocatalysis and Structural Effects on the Rate of Nitric Oxide Release. *J. Phys. Chem. A* **2002**, *106* (38), 8963–8970.

(47) Szaciłowski, K.; Stasicka, Z. S-Nitrosothiols: Materials, Reactivity and Mechanisms. *Prog. React. Kinet. Mech.* **2001**, *26*, 1–58.

(48) Williams, D. L. The Chemistry of S-Nitrosothiols. *Acc. Chem. Res.* **1999**, *32* (10), 869–876.

(49) Aronow, R.; Fleischmann, L. E. Mercury Poisoning in Children. The Value of N-Acetyl-D,L-Penicillamine in a Combined Therapeutic Approach. *Clin. Pediatr. (Philadelphia)* **1976**, *15* (10), 936–937 943–945..

(50) Jones, M. M.; Weaver, A. D.; Weller, W. L. The Relative Effectiveness of Some Chelating Agents as Antidotes in Acute Cadmium Poisoning. *Res. Commun. Chem. Pathol. Pharmacol.* **1978**, *22* (3), 581–588.

(51) Kark, R. A.; Poskanzer, D. C.; Bullock, J. D.; Boylen, G. Mercury Poisoning and Its Treatment with N-Acetyl-D,L-Penicillamine. *N. Engl. J. Med.* **1971**, *285*, 10–16.

(52) Parameshvara, V. Mercury Poisoning and Its Treatment with N-Acetyl-D,L-Penicillamine. *Occup. Environ. Med.* **1967**, *24*, 73–76.

(53) Srivastava, P.; Arif, A. J.; Singh, C.; Pandey, V. C. N-Acetylpenicillamine a Protector of Plasmodium Berghei Induced Stress Organ Injury in Mice. *Pharmacol. Res.* **1997**, *36* (4), 305–307.

(54) Graeme, K. A.; Pollack, C. V. Heavy Metal Toxicity, Part I: Arsenic and Mercury. *J. of Emerg. Med.* **1998**, *16*, 45–56.

(55) Arulسامي, N.; Bohle, D. S.; Butt, J. A.; Irvine, G. J.; Jordan, P. A.; Sagan, E. Interrelationships between Conformational Dynamics and the Redox Chemistry of S-Nitrosothiols. *J. Am. Chem. Soc.* **1999**, *121* (30), 7115–7123.